Potential of carbon uptake and local aerosol production in boreal and hemi-boreal ecosystems across Finland and in Estonia

Piaopiao Ke[1], Anna Lintunen[1,2], Pasi Kolari[1], Annalea Lohila[1,3], Santeri Tuovinen[1], Janne Lampilahti[1], Roseline Thakur[1], Maija Peltola[1], Otso Peräkylä[1], Tuomo Nieminen[1], Ekaterina Ezhova[1], Mari Pihlatie[2,4], Asta Laasonen[1], Markku Koskinen[2,4], Helena Rautakoski[3], Laura Heimsch[3], Tom Kokkonen[1], Aki Vähä[1], Ivan Mammarella[1], Steffen Noe[5], Jaana Bäck[2], Veli-Matti Kerminen[1], and Markku Kulmala[1]

[1]Institute for Atmospheric and Earth System Research (INAR)/Physics, Faculty of Science, University of Helsinki, Helsinki, 00014, Finland
[2]Institute for Atmospheric and Earth System Research (INAR)/Forest Sciences, Faculty of Agriculture and Forestry, University of Helsinki, Helsinki, 00014, Finland
[3]Climate System Research, Finnish Meteorological Institute, Helsinki, 00101, Finland
[4]Department of Agricultural Sciences, Faculty of Agriculture and Forestry, University of Helsinki, Helsinki, 00790, Finland
[5]Institute of Forestry and Engineering, Estonian University of Life Sciences, Tartu, 51006, Estonia

Correspondence: Piaopiao Ke (piaopiao.ke@helsinki.fi) and Markku Kulmala (markku.kulmala@helsinki.fi)

Received: 27 June 2024 – Discussion started: 26 July 2024
Revised: 26 February 2025 – Accepted: 28 March 2025 – Published:

Abstract. Continental ecosystems play an important role in carbon dioxide (CO_2) uptake and aerosol production, which help to mitigate climate change. The concept of "CarbonSink+ potential" enables a direct comparison of CO_2 uptake and local aerosol production at the ecosystem scale. Following this concept, momentary net ecosystem exchange (NEE) and the number concentration of negative intermediate ions at 2.0–2.3 nm (N_{neg}) were analysed for boreal and hemi-boreal ecosystems across Finland and in Estonia. N_{neg} can tell us how effectively gaseous precursors associated with biogenic emissions from an ecosystem initiate the new particle formation. Four forests, three agricultural fields, an open peatland, an urban garden, and a coastal site were included, with a focus on the summertime. We compared the NEE and N_{neg} at each site to the boreal Hyytiälä forest (F-HYY) as it is constituted by the dominant ecosystem type in Finland. N_{neg} was highest at the urban garden site and lowest at the coastal site. The agricultural fields had higher or similar net CO_2 uptake rates and higher N_{neg} than all studied forests. The median net CO_2 uptake rate of the open peatland was only 31 % of that at F-HYY, while the median N_{neg} was 77 % of that at F-HYY. The median net CO_2 uptake rate in the urban garden was 63 % of that at F-HYY, implying the importance of urban green areas in CO_2 storage. The coastal site was a minor CO_2 sink. It should be noted that the harvest biomass in agricultural fields is not accounted for in this study. Given the large area of forests in Finland, the forests are the most important ecosystems in terms of their CO_2 uptake and local aerosol formation with regard to helping to mitigate climate warming.

1 Introduction

Carbon dioxide (CO_2) is one of the most abundant greenhouse gases in the atmosphere and the most important cause of global warming (e.g. Jia et al., 2022). Terrestrial ecosystems play an essential role in the global CO_2 budget through carbon uptake from the atmosphere by means of photosynthesis and its consequent sequestration to various pools (Walker et al., 2021; Friedlingstein et al., 2022). Globally, the net terrestrial ecosystem uptake of CO_2 (i.e. the net carbon sink) is 3.1 Gt C yr^{-1}, which accounts for 32 % of CO_2 emissions from fossil fuel combustion (Friedlingstein et al., 2022). Terrestrial carbon sequestration, i.e. the process of storing carbon in a carbon pool (IPCC, 2022), takes place in both belowground and aboveground carbon storage (Walker et al., 2021, and the reference therein). Belowground storage

includes soil carbon pools, while aboveground storage is primarily in the form of biomass. As a transition between land and open ocean, the coastal environment is identified as an import carbon sink and is estimated to take up $0.4\,\mathrm{Gt\,C\,yr^{-1}}$ (Regnier et al., 2022). Large spatiotemporal variations in continental CO_2 uptake are assumed due to different ecosystem and land use types, climatic conditions, and management pathways (Chang et al., 2021; Friedlingstein et al., 2022). The challenge of increasing the carbon sequestration of ecosystems has been attracting more and more attention, with the global goal of reducing CO_2 concentrations in the atmosphere.

Apart from acting as CO_2 sinks, terrestrial ecosystems can influence climate by contributing to the formation of new aerosol particles (Kulmala et al., 2004; Kulmala et al., 2014; Kulmala et al., 2020; Yli-Juuti et al., 2021; Junninen et al., 2022; Petäjä et al., 2022, Räty et al., 2023). Globally, aerosols have been reported to induce a net climate cooling effect. The best estimate of the effective radiative forcing is $-1.06\,\mathrm{W\,m^{-2}}$ (Jia et al., 2022). However, large uncertainties exist in the aerosol net radiative forcing estimation, tightly associated with the large spatiotemporal heterogeneity in its origin, number concentration, and chemical properties.

Atmospheric new particle formation (NPF) is an important source of cloud condensation nuclei (CCN) (e.g. Gordon et al., 2017; Ren et al., 2021; Zhang et al., 2023) which contributes significantly to aerosol–cloud and aerosol–radiation interactions (Rosenfeld et al., 2014; Ezhova et al., 2018, Artaxo et al., 2022; Petäjä et al., 2022). NPF takes place frequently in many environments, such as forests, urban cities, and coastal areas (e.g. Kerminen et al., 2018; Nieminen et al., 2018; Zheng et al., 2021). It has been reported that NPF is greatly enhanced due to the emission of biogenic volatile organic compounds (BVOCs) in boreal forests and peatlands (Junninen et al., 2022; Petäjä et al., 2022). Notably, NPF events often take place regionally, extending over distances of up to over 1000 km (Kerminen et al., 2018). Multiple types of ecosystems may contribute to the NPF events in a region, depending, for example, on the diversity of land use types. It remains unclear whether and how various ecosystems differ in terms of their contributions to regional NPF and what the magnitude of such differences is.

To overcome the challenge of analysing the role of local ecosystems in regional aerosol formation, the concept of "CarbonSink+ potential" was recently established (Kulmala et al., 2024). CarbonSink+ potential enables a direct, ecosystem-scale comparison of CO_2 uptake and the intensity of local intermediate ion formation (LIIF) in the atmosphere at the ecosystem scale. The LIIF can be approximated as the number concentration of negative intermediate ions in the 2.0–2.3 nm size range (Tuovinen et al., 2024) to which the aerosol formation in the 3–6 nm size range is proportional (Kulmala et al., 2024). The survival probability of small aerosol particles, which describes the probability of a single particle growing to a certain size without being scavenged, is generally high for particles from 6 nm to CCN size in rural and remote environments (Kulmala et al., 2024; Stolzenburg et al., 2023). The local contributions of certain ecosystems to regional aerosol formation can thus be quantified by LIIF.

This study utilized 1- to 10-year-long datasets of intermediate ion concentrations and CO_2 fluxes from various boreal and hemi-boreal ecosystems across Finland and in Estonia. In summary, four forests, one open peatland, three agricultural fields, one urban garden, and one coastal site were investigated. The negative intermediate ion concentrations and CO_2 fluxes for these ecosystems were compared during different seasons, with a focus on the summer. Based on the CarbonSink+ potential concept (Kulmala et al., 2024), the potential of these ecosystems to mitigate climate warming in relation to CO_2 uptake and aerosol production is discussed.

2 Method

2.1 Site description

In this study, various ecosystem types, including forests, open peatland, agricultural fields, coastal areas, and an urban garden were studied (Fig. 1; Table 1). All stations utilize the SMEAR (Station for Measuring Ecosystem–Atmosphere Relations; Hari and Kulmala, 2005) concept. The detailed location, ecosystem type, meteorological characteristics, and soil type for each site are presented in Table 1. SMEAR I in Värriö in northern Finland (F-VAR) and SMEAR II in Hyytiälä in southern Finland (F-HYY) are forest sites, both dominated by Scots pine (Kulmala et al., 2019; Neefjes et al., 2022), while the forests in Ränskälänkorpi (F-RAN) and at the SMEAR site in Estonia at Järvselja (F-JAR) are mixtures of coniferous and broadleaf trees (Table 1). While F-VAR and F-HYY are upland forests, i.e. growing on mineral soil, F-RAN is a drained-peatland forest (Laurila et al., 2021), and F-JAR has a mosaic of drained swamp, drained peat, and leached gleyic pseudo-podzols (Kangur et al., 2021; Noe et al., 2015). Two of the agricultural (SMEAR-Agri) sites, i.e. Haltiala (A-HAL), a cereal cropland, and Viikki (A-VII), a managed grassland which was renewed in 2023 with a cereal crop, are located in Helsinki. The third agricultural site, Qvidja (A-QVI), is a managed grassland located in southwestern Finland (Heimsch et al., 2021). The SMEAR II site at Siikaneva (P-SII) is an open, pristine peatland site ~ 5 km southwest of F-HYY (Rinne et al., 2018). SMEAR III at Kumpula, Helsinki, is an urban background site. The University of Helsinki botanical garden and the city of Helsinki allotment garden are in the southwest of the SMEAR III station, characterized by a high fraction of vegetation (G-KUM; Järvi et al., 2012). The coastal site (C-TVA) is at Tvärminne Zoological Station, which is a 600 ha nature reserve at the entrance of the Gulf of Finland (northern Baltic Sea), southwestern Finland (Virtasalo et al., 2023). During the measurement period, the annual mean temperature for these sites

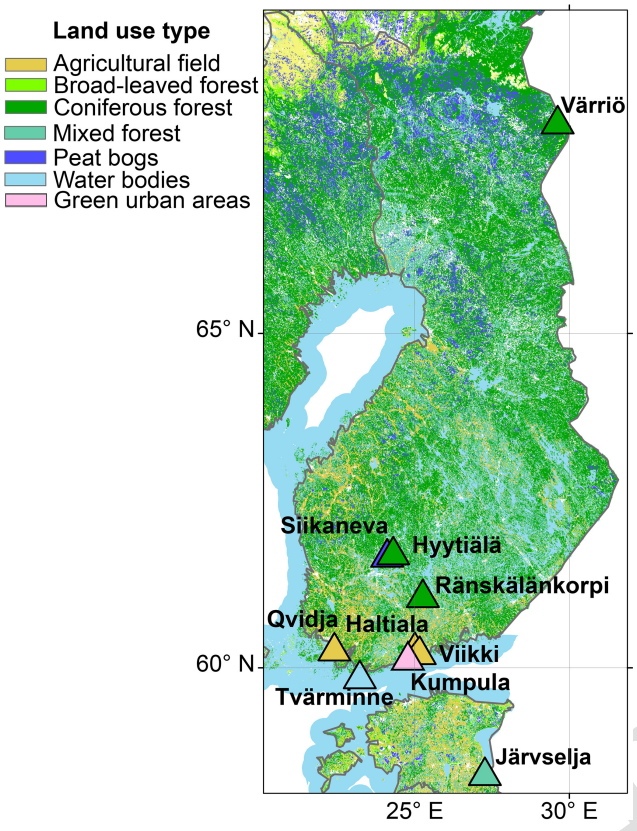

Figure 1. Land type distribution across Finland (Copernicus Global Land Service, 2020) and the studied sites, with their ecosystem type shown.

ranged between 0.4 and 7.2 °C, while the annual precipitation ranged between 500 and 750 mm (Table 1). F-JAR, C-TVA, and A-QVI belong to hemi-boreal ecosystems, while the other ecosystems are boreal (Mäki et al., 2022).

2.2 Atmospheric measurements: intermediate ions, CO_2 flux, and meteorological parameters

The number concentration of ions and particles and the net ecosystem exchange (NEE) of CO_2 were measured using a neutral cluster and air ion spectrometer (NAIS, Airel Ltd; Mirme and Mirme, 2013) and an eddy covariance method (Aubinet et al., 1999), respectively. The meteorological data, e.g. air temperature, air humidity, and photosynthetic photon flux density (PPFD), were measured simultaneously at the same heights with the eddy covariance setup. If the meteorological measurement at the same height (Table S1 in the Supplement) was not available, it was replaced by the one from the next nearest height. The types of analysers and detectors used at each site are listed in Table S1.

The NAIS is capable of continuous monitoring of ion and total particle concentrations and size distributions over the diameter range of 0.8–42 nm. The ions can be divided into three different size ranges, namely small ions (also referred to as cluster ions) in the sub-2 nm size range, intermediate ions (2–7 nm), and large ions (>7 nm; Tammet et al., 2014). The time resolution was set to 5 min to optimize the signal-to-noise ratio (Mirme and Mirme, 2013). The data were quality-checked, considering, for example, the potential interference of rainfall and snow events in the measurements (Manninen et al., 2016). The ion and total particle number concentration were further averaged over half an hour. The inlets for the NAIS at all of the studies sites are 1–2 m a.g.l. (above ground level).

In this study, we identified the concentration of negative intermediate ions, specifically within the range of 2.0–2.3 nm (N_{neg}), as an indicator of the local intermediate ion formation (LIIF). It is important to note that the intensity of LIIF can serve as an estimate of the local contribution to the regional NPF (Kulmala et al., 2024). It has been observed that N_{neg} displays distinct differences between new particle formation and non-formation periods of intermediate ions (2–7 nm; Tuovinen et al., 2024), thereby making N_{neg} a reliable indicator of LIIF. Moreover, the measurement of negative intermediate ions between 2.0 and 2.3 nm by the NAIS provides a relatively high degree of accuracy, and the measurement footprints are constrained to be within the ecosystem scale when measured under the canopy (sub-1 km; Tuovinen et al., 2024; Kulmala et al., 2024). Moreover, the median values of N_{neg} between 00:00 and 06:00 LT (local time), i.e. outside the active hours of the ecosystem, were taken as the background concentration at each site. The background value of N_{neg} was calculated separately for each season. A narrower time window for background concentrations compared to the one proposed by Aliaga et al. (2023), namely 21:00–06:00 LT, was applied due to the more northern F-VAR, with a longer day length during the summer in this study. We then calculated the changes in N_{neg} (ΔN_{neg}) by subtracting the background concentration during each season from N_{neg}. The diurnal variations in median ΔN_{neg} were presented together with N_{neg} (Sect. 3). The use of ΔN_{neg} was assumed to eliminate the influence of background clustering at different sites (Aliaga et al., 2023) such that it reflects the intensity of negative intermediate ion production from the specific ecosystem.

The eddy covariance measurement of CO_2 fluxes is based on the turbulence theory, i.e. the assumption that the turbulent flux remains relatively stable in a constant flux layer above the canopy (Lee and Hu, 2002), and it is equal to the covariance of vertical wind speed and ambient CO_2 concentration on flat and horizontally homogeneous surfaces (Aubinet et al., 1999). The fluxes were measured above the ecosystem canopies and below 30 m. The detailed measurement height for each site is listed in Table S1. The measurement system requires a fast-response analyser of the CO_2 concentration (10 Hz) and a 3-D sonic anemometer. The raw eddy covariance 10 Hz data were pre-processed with standard steps, including despiking, detrending, dilution correction, and 2-D coordinate rotation (Aubinet et al., 1999). The

Table 1. Meteorological and other main characteristics of the studied sites.

Sites (site ID)		Location	Selected period (mm/yyyy)	Mean air temperature (°C)	Rainfall (mm yr^{-1})	Dominant plant species	Peak LAI	Climate zone
Forest	Hyytiälä, SMEAR II (F-HYY)	61°51′ N, 24°17′ E	11/2009–12/2022	4.8	709[1]	Scots pine and Norway spruce	4.6	Boreal
	Värriö, SMEAR I (F-VAR)	67°46′ N, 29°35′ E	3/2019–12/2022	0.4	601[2]	Scots pine	3.2	Boreal
	Ränskälänkorpi (F-RAN)	61°10′ N, 25°16′ E	4/2021–12/2022	5.4	600[3]	Norway spruce, Scots pine, downy birch	–	Boreal
	Järvselja, SMEAR Estonia (F-JAR)	58°16′ N, 27°16′ E	10/2016–12/2020	6.8	500–750[4]	Birch species, Scots pine, Norway spruce	6	Hemi-boreal
Agricultural fields	Haltiala, SMEAR-Agri (A-HAL)	60°16′ N, 24°57′ E	6/2021–10/2022	6.5	700[5]	Oat	5.5	Boreal
	Qvidja (A-QVI)	60°18′ N, 22°24′ E	12/2018–8/2022	7.0	679[6]	Timothy, meadow fescue	6.2	Hemi-boreal
	Viikki, SMEAR-Agri (A-VII)	60°13′ N, 25°01′ E	7/2022–6/2023	6.5	792[5]	Timothy (2022), barley (2023)	5.2	Boreal
Peatland	Siikaneva, SMEAR II (P-SII)	61°50′ N, 24°12′ E	11/2019–12/2022	5.0	710[7]	Moss and sedges	0.6	Boreal
Urban garden	Kumpula, SMEAR III (G-KUM)	60°12′ N, 24°58′ E	5/2016–12/2022	6.3[5]	731[5]	Mixed	–	Boreal
Coastal area	Tvärminne (C-TVA)	59°51′ N, 23°15′ E	6/2022-8/2023	7.2[5]	639[5]	Seagrass and seaweed	–	Hemi-boreal

[1] Neefjes et al. (2022). [2] Kulmala et al. (2019). [3] Laurila et al. (2021). [4] Noe et al. (2015). [5] Finnish Meteorology Institute – only data for the same calendar year of the selected period and for the same or nearby stations as NAIS and eddy covariance measurements were applied. [6] Heimsch et al. (2021). [7] Rinne et al. (2018) – data not available.

fluxes were further lag-time-adjusted and corrected for spectral loss (Aubinet et al., 1999). Either EddyUH (Mammarella et al., 2016) or EddyPro (Fratini and Mauder, 2014) or the programme introduced by Heimsch et al. (2021) was applied for the pre-processing for one site. The processed fluxes were accepted only if they met the stationarity and developed turbulence criterion (Foken and Wichura, 1996), exceeding the site-specific friction velocity thresholds (Table S1). The quality-checked CO_2 fluxes at the forest sites were further partitioned into gross primary production (GPP) and ecosystem respiration (R) using the site-specific dependence of R on the air and/or soil temperature and of GPP on the PPFD and air and/or soil temperature (Kulmala et al., 2019).

2.3 Data selection criteria

In this study, the analyses were restricted to periods when both negative intermediate ion concentration and NEE were available (Table 1). Therefore, different time periods were applied for each of the different sites. For F-HYY, F-VAR, F-JAR, F-QVI, P-SII, and G-KUM, the long-term data were available for more than 3 years. At F-HYY, 12 years of continuous observations were used. For the sites with recently established atmospheric measurements, namely C-TVA, F-RAN, A-HAL, and A-VII, data were available for approximately 1 to 1.5 years. In total, 35 site years of data were utilized in this study. As we focused on the potential of the ecosystem to take up CO_2 and form intermediate ions, the inter-annual variation at the sites was not discussed in this study (Kulmala et al., 2019; Alekseychik et al., 2021; Heimsch et al., 2021).

F-HYY had the longest data recordings (Table 1) among the 10 sites and received relatively little anthropogenic pollution (Neefjes et al., 2022). Due to the thinning of F-HYY in the beginning of the year 2020, when 40 % of tree basal area was removed (Aalto et al., 2023), data from that year were discarded from the analyses to exclude the immediate thinning effect on the studied variables. At F-RAN, the western part of the site was selectively harvested (~ 60 % of basal area removed), and the eastern part of the site was clear-cut in the spring and summer of 2021, with a control site left in the middle. The NAIS equipment was positioned on the border between the control and clear-out, ~ 230 m east from the eddy covariance tower (measurement height of 29 m). The eddy covariance tower was on the border between the control and selectively harvested plots. In this study, only data with wind blowing from the area after selective harvesting from the west (WD $> 180°$) and with wind speed above $2\,\mathrm{m\,s^{-1}}$ were considered. Note that carbon removed from the site in harvested tree biomass is not accounted for in the measured flux of CO_2. At G-KUM, data from the garden area, i.e. 180–320°, were applied. The vegetation varied largely, from broadleaf forests to gardens (Järvi et al., 2012).

At the agricultural sites, the management activity is relatively intense and can distinctly influence the CO_2 fluxes (Heimsch et al., 2021). Note that the carbon removed in harvested crop biomass and the carbon added to the site in fertilizers do not directly contribute to the measured net flux of CO_2. For A-QVI, NAIS and eddy covariance data from wind directions of 30 to 140° were discarded due to another separated experimental plot located in that part of the field (Heimsch et al., 2021). Also, the data were discarded when the flux footprint was not sufficiently representative of the target grassland (Heimsch et al., 2021). Similarly, at A-VII, only measurements from wind directions between 145 and 245° were included in the analysis to avoid data from other nearby fields with different vegetation and management activities. A-QVI was harvested in June and August, A-VII was harvested twice in August during the reported period, and A-HAL was harvested once only at the end of the growing season during the measurement periods. The sowing (overseeding for A-QVI and only in 2022) and first fertilization in the year usually take place at the end of spring.

The open peatland at P-SII is surrounded by forests. However, 80 % of the CO_2 flux footprint is within ~ 150 m from the measurement tower, i.e. constrained within the peatland (Alekseychik et al., 2021). At C-TVA, the NAIS instrument trailer is on the shore, and the eddy covariance mast is on an island, ~ 110 m east of the shore. Only data with wind directions from 95 to 165° and from 205 to 240°, i.e. from the coastal water without being disturbed by trees on nearby islands, were included in the analysis at this site.

3 Results and discussion

3.1 Comparison of momentary NEE in different ecosystems

The diurnal variations in NEE between the studied forests, urban garden area, agricultural fields, open peatland, and coastal site in spring (MAM) and summer (JJA) are presented in Figs. 2–4. The corresponding comparisons with autumn (SON) and winter (DJF) are presented in Figs. S1–S3.

For the forest sites, the hemi-boreal F-JAR tended to have the highest net CO_2 uptake rate (absolute values of NEE when it is negative) at midday (10:00–14:00 LT) in both spring and summer. The median net CO_2 uptake rate at midday at F-JAR reached $12\,\mu\mathrm{mol\,m^{-2}\,s^{-1}}$ in summer. The lowest net CO_2 uptake rate at midday was found at the most northern F-VAR, with the median being $4.69\,\mu\mathrm{mol\,m^{-2}\,s^{-1}}$. This difference may be due to the 6–8 °C higher air temperature in the hemi-boreal Estonian forest and the lower temperature at F-VAR (Fig. S4) as the ecosystem productivity at high latitudes in Europe is typically temperature limited (Yi et al., 2010).

In summer, the net CO_2 uptake rate in the urban garden area at G-KUM was comparable with the drained-peatland forest at F-RAN. The vegetation fraction at G-KUM is relatively high (0.44). During summertime, the strong photo-

synthesis dominated the changes in CO_2 fluxes, inducing a net CO_2 uptake in the garden section (Järvi et al., 2012). In the other seasons, the urban garden area was a net source of CO_2 most of the time (Figs. 2 and S1), similarly to the results previously reported for the years 2006–2010 from the same site (Järvi et al., 2012). There are residential buildings and traffic within the eddy covariance measurement footprint at G-KUM. The CO_2 emissions from the residential buildings, traffic, and soils outweighed photosynthetic uptake of CO_2, except during the daytime in summer.

In the case of agricultural fields in summer (Fig. 3), the A-HAL and A-VII croplands had 2–5 $\mu mol\,m^{-2}\,s^{-1}$ (for the median values at midday) higher momentary net CO_2 uptake rate than A-VII. Notably, in spring, the croplands at A-VII and A-HAL were net sources of CO_2, while A-QVI was a CO_2 sink during the daytime, with an uptake rate comparable to that at F-HYY (ranging between 0 and 4 $\mu mol\,m^{-2}\,s^{-1}$). The different plant species (Table 1) and management activities between the agricultural fields are likely to have caused the differences in their seasonal CO_2 fluxes. During the measurement period, perennial grass species were grown at A-QVI, while the growth of the annual crops at A-HAL and A-VII relied on the sowing and fertilization date, normally at the end of spring. This may explain the springtime CO_2 emission at A-HAL and A-VII. In the summer, A-HAL and A-VII were harvested only in August, while A-QVI was harvested in June and August separately, which may explain the higher CO_2 uptake rate at A-HAL and A-VII. The upper quartile of the momentary net CO_2 uptake, i.e. absolute values of 25th percentile NEE, was 62 % higher at A-HAL than that at F-HYY in summer. The midday momentary net CO_2 uptake rate at A-VII was 17 % higher than that at F-HYY, while that at A-QVI was 30 % lower than that at F-HYY. It is also important to note that the harvests of plant biomass decreased local carbon storage, which was not accounted for in the measured CO_2 fluxes. In the studied agricultural fields, the harvest was conducted once or twice every year, whereas the typical rotation lengths in managed boreal areas are 60–100 years in southern Finland.

The CO_2 uptake rate and respiration rate (nighttime CO_2 fluxes) in the open peatland (P-SII) and coastal area (C-TVA) (Fig. 4) were distinctly lower than those in the agricultural fields and forests during spring and summer. Still, the P-SII remained a net sink of CO_2 during the daytime in all the seasons except for winter. The midday NEE values at C-TVA were -0.25 and -0.01 $\mu mol\,m^{-2}\,s^{-1}$ in spring and summer, respectively. Hence, stronger net CO_2 uptake possibly appears in spring in this Baltic coastal area under certain conditions, i.e. when the partial pressure of CO_2 in the water is lower than that in the air (Roth et al., 2023). This may be induced by fast growth of phytoplankton and submerged vegetation in the spring (Roth et al., 2023).

Additionally, F-RAN and F-JAR turned into a CO_2 source 1–2 h earlier in the late afternoon during summer than the other two forests (Fig. 2). Note that the soil at F-RAN and F-JAR is mainly drained peatland and water-logged soil (Table 1), respectively, which is indicated by a high organic carbon content (Laurila et al., 2021; Noe et al., 2015). The elevated air temperature (Fig. S4) and increased soil organic carbon content may contribute to the enhanced respiration at the two sites, which is reflected in the nighttime fluxes (Fig. 2). Hence, even though the GPP values at F-JAR and F-RAN in the late afternoon were close to that at F-HYY (Fig. 5), net emissions of CO_2, i.e. positive NEE values, were observed at these two forest sites in the earlier and later hours of the day.

3.2 Comparison of negative intermediate ion concentrations across different ecosystems

The comparisons of N_{neg} between different ecosystems in spring and summer are presented in Figs. 6–8. It was assumed that negative intermediate ions at 2.0–2.3 nm can describe how efficiently the ecosystem can produce new aerosol particles (Kulmala et al., 2024; Tuovinen et al., 2024). The corresponding values of N_{neg} in autumn and winter were only 16 %–84 % of those in spring and summer (Figs. S5–S7). The N_{neg} values in the daytime during spring were significantly higher than those in the summer at A-HAL and G-KUM (Mann–Whitney U test based on daily medians, $P<0.05$). At F-VAR, F-HYY, and F-RAN, the median values in summer were significantly higher than those in spring ($P<0.05$). For other sites, the difference was not significant ($P>0.05$). In contrast, the difference between the 75th and 50th percentiles of N_{neg} in spring was higher than that in summer at all the studied sites except F-VAR and C-TVA. The larger upper-quartile deviation of N_{neg} in spring implied that the LIIF processes were either more frequent or stronger in spring than in summer at all the sites except F-VAR and C-TVA (Dada et al., 2018; Nieminen et al., 2018).

For all the sites, the diurnal variation in negative intermediate ions in spring and summer was clear, except for C-TVA in spring, i.e. a distinct peak during the daytime. In the winter, the diurnal cycle of N_{neg} was not visible at any of the studied sites (Figs. S6–S8). This agrees with the observation that the global radiation and air temperature are observed to correlate positively with the concentration of negative intermediate ions at 2–4 nm at F-HYY (Neefjes et al., 2022).

The daily fluctuations of N_{neg} (ΔN_{neg}) were calculated by subtracting the background concentration from N_{neg} in each season (Sect. 2.2). In spring, median ΔN_{neg} at midday for the forests ranged between 0.8 and 2.0 cm^{-3} (Table S2), with the lowest value at F-JAR and the highest value at F-HYY. The midday mean ΔN_{neg} at G-KUM was 4.9 cm^{-3}, which was 2–7 times that in the studied forests. The presence of more abundant nucleation precursors at G-KUM may facilitate the ion formation (Nieminen et al., 2018). Seasonal changes in the clustering precursors and their dependence on air temperature and radiation may drive the seasonal variation in ΔN_{neg} at all of the sites.

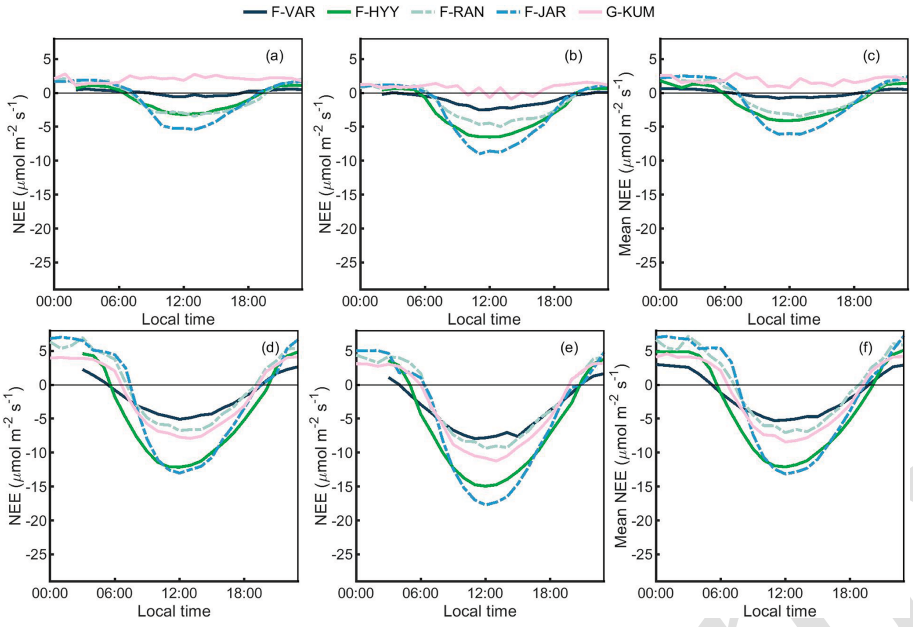

Figure 2. The 50th percentile **(a)**, 25th percentile **(b)**, and mean values **(c)** of NEE at each hour for the forest sites and urban garden in spring (MAM) and the corresponding 50th percentile **(d)**, 25th percentile **(e)**, and mean values **(f)** in summer (JJA).

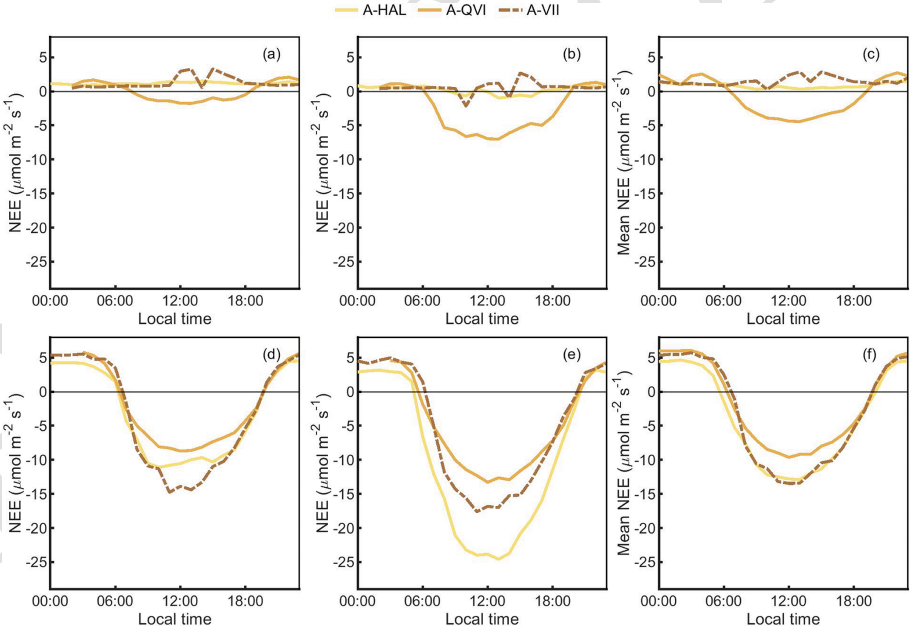

Figure 3. The 50th percentile **(a)**, 25th percentile **(b)**, and mean values **(c)** of NEE at each hour for the agricultural fields in spring (MAM) and the corresponding 50th percentile **(d)**, 25th percentile **(e)**, and mean values **(f)** in summer (JJA).

It is notable that, generally, the agricultural sites had higher midday ΔN_{neg} than the forest sites in spring, varying between 2.3 and 7.7 cm^{-3}. The application of fertilizers is known to increase the atmospheric concentration of ammonia (NH_3) remarkably in agricultural fields, e.g. as observed at A-QVI (Olin et al., 2022). NH_3 can stabilize the critical clusters in the nucleation process driven by sulfuric acid (H_2SO_4). H_2SO_4 in the air is formed majorly by oxidation of sulfur dioxide, which can be transported over a longer range than the intermediate ions. However, the frequency of NPF events was found not to increase after the fertilization at A-QVI (Dada et al., 2023). Similarly, the frequency of daytime NPF events did not correlate with agriculture activities in a cropland in France (Kammer et al., 2023). Dada et al. (2023)

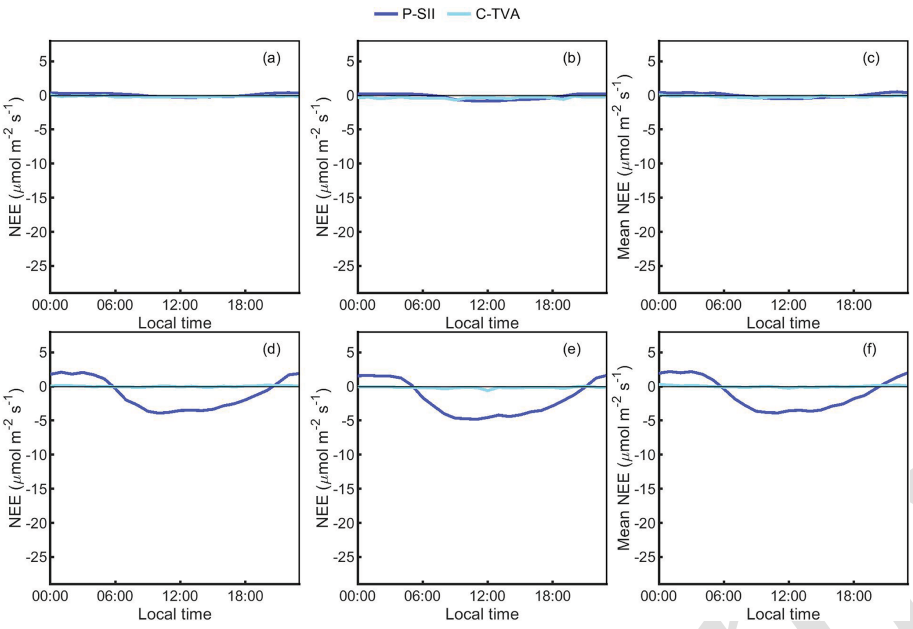

Figure 4. The 50th percentile **(a)**, 25th percentile **(b)**, and mean values **(c)** of NEE at each hour for the peatland and coastal area in spring (MAM) and the corresponding 50th percentile **(d)**, 25th percentile **(e)**, and mean values **(f)** in summer (JJA).

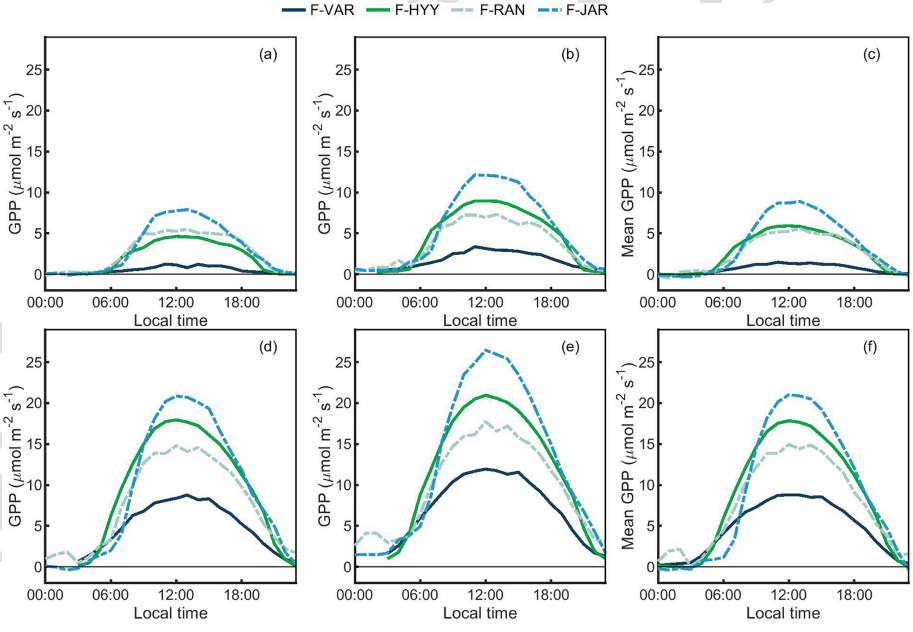

Figure 5. The 50th percentile **(a)**, 75th percentile **(b)**, and mean values **(c)** of GPP at each hour for the forest sites in spring (MAM) and the corresponding 50th percentile **(d)**, 75th percentile **(e)**, and mean values **(f)** in summer (JJA).

observed that NH_3, H_2SO_4, and low volatile organic compounds originating from BVOC oxidation play a synergistic role in clustering at A-QVI, resulting in a 7–57-times and 2–16-times higher formation rate and number concentration of particles, respectively, than at F-HYY. Note that, since the A-HAL and A-VII croplands are located in Helsinki, the nucleation precursors and, thereby, the nucleation rate may be enhanced by anthropogenic pollution in the city. The exact reasons why there were higher N_{neg} and ΔN_{neg} rates at these agricultural sites require exploration through more measurements of the clustering precursors.

Furthermore, in spring and summer, the nighttime N_{neg} increased again at around 20:00 LT for all the sites, suggesting a ubiquitous nighttime clustering in warm seasons (Ma-

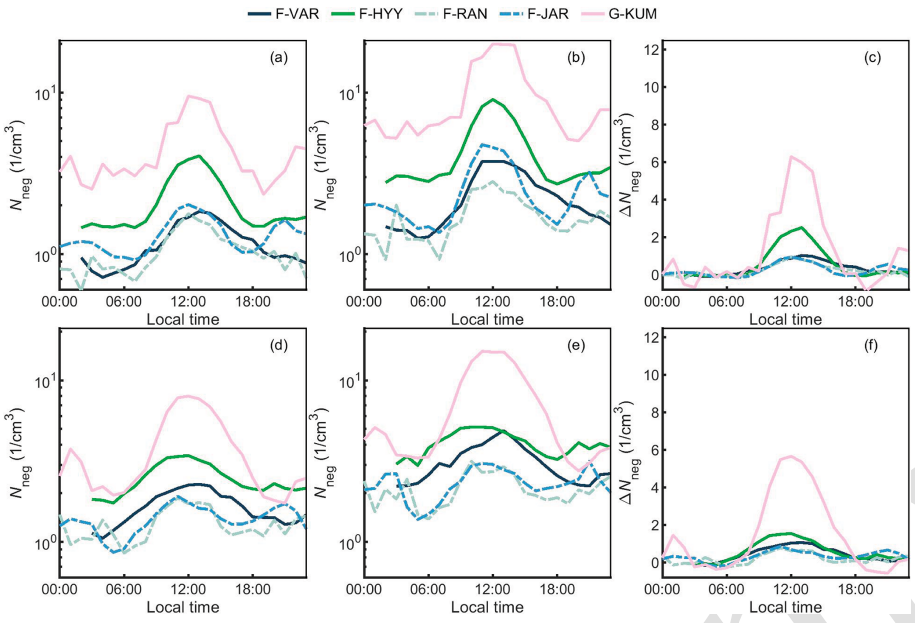

Figure 6. The 50th percentile **(a)** and 75th percentile **(b)** of negative intermediate ions (N_{neg}) at 2.0–2.3 nm (N_{neg}) at each hour and the daily fluctuations of N_{neg} **(c)** for the forests and urban garden in spring (MAM) and the corresponding 50th percentile **(d)**, 75th percentile **(e)**, and normalized concentration for median values **(f)** in summer (JJA).

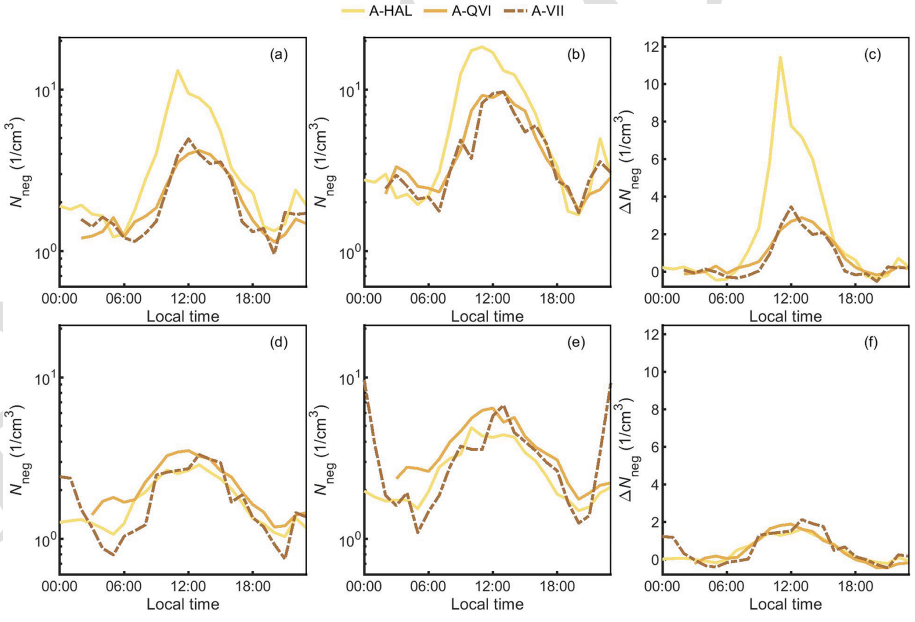

Figure 7. The 50th **(a)** and 75th percentile **(b)** of negative intermediate ions (N_{neg}) at 2.0–2.3 nm at each hour and the daily fluctuations of N_{neg} **(c)** for the agricultural fields in spring (MAM) and the corresponding 50th percentile **(d)**, 75th percentile **(e)**, and normalized concentration for median values **(f)** in summer (JJA).

zon et al., 2016). However, these nighttime-clustered negative ions are likely to be unable to grow >3 nm in diameter (Mazon et al., 2016). Moreover, in summer, the 75th percentile of nighttime N_{neg} at A-VII was comparable with the daytime N_{neg}. The decreased boundary layer height (Chen et al., 2016; Neefjes et al., 2022), especially during clear nights, may also facilitate the accumulation of formed clusters and eventually lead to the nighttime peak.

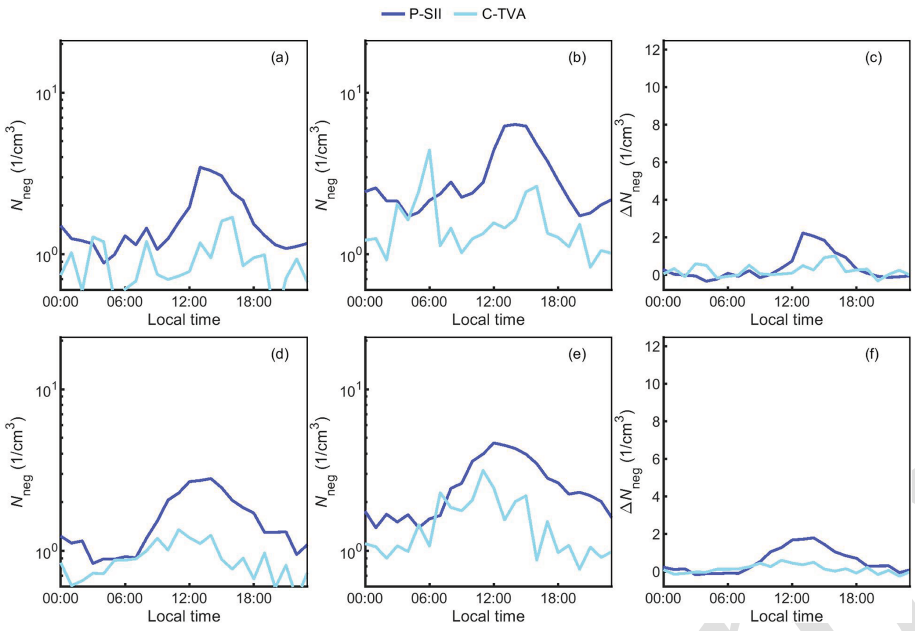

Figure 8. The 50th percentile **(a)** and 75th percentile **(b)** of negative intermediate ions (N_{neg}) at 2.0–2.3 nm at each hour and the daily fluctuations of N_{neg} **(c)** for the peatland and coastal area in spring (MAM) and the corresponding 50th percentile **(d)**, 75th percentile **(e)**, and normalized concentration for median values **(f)** in summer (JJA).

3.3 Potential of different ecosystems to contribute to CO_2 uptake and negative intermediate ion production

Since we aimed to compare the potential of ecosystems for net CO_2 uptake and local production of negative intermediate ions (LIIF), the most active periods for the ecosystem plants are discussed in detail in this section, i.e. midday in summertime. The potential of the studied ecosystems for net CO_2 uptake and LIIF at midday during summertime is listed in Table 2. The values of NEE and N_{neg} at F-HYY were also used as references to which NEE and N_{neg} at all other sites were compared (Table 2). For median values in summer, N_{neg} was found to be highest in the urban garden, followed by the agricultural fields (Fig. 9). The agricultural fields generally had higher N_{neg} than the studied forests, and the open peatland (P-SII) had 23 % lower N_{neg} than F-HYY but 15 %–46 % higher N_{neg} than the other forests. The N_{neg} at the coastal area was the lowest. The momentary net CO_2 uptake rate at midday in summer was highest in agricultural fields, followed by the forests. The urban garden in this study displayed distinct net CO_2 uptake which was 37 % lower than in the forests and ∼2 times that in the open peatland. The coastal area at midday in summer was a very weak CO_2 sink. In the urban garden area at G-KUM, the median N_{neg} was double that at F-HYY, while the median NEE only reached 63 % of that at F-HYY.

The variations in momentary NEE and N_{neg} were distinct, even between similar types of ecosystems at a similar latitude (Sect. 3.1 and 3.2), e.g. within forests and agricultural fields. For forests, the most southern F-JAR had the highest net CO_2 uptake rate, while the median N_{neg} at midday in summer was similar to that at F-RAN and 53 % of that at F-HYY. F-HYY had higher N_{neg} than the other forests. For agricultural sites, the net CO_2 uptake rates at A-VII and A-HAL were close to that at F-HYY, while they were 30 % lower at A-QVI than at F-HYY. On the contrary, the N_{neg} values were highest at A-QVI between the three agricultural sites, and the median N_{neg} values of the other two croplands were 12 %–19 % smaller than at F-HYY.

Multiple factors can cause the differences in NEE and N_{neg} across the sites despite the similar seasonal and diurnal variation patterns. The CO_2 uptake rate at midday in summer increased with an increasing air temperature in both studied forests and agricultural fields (Fig. 9). Moreover, the CO_2 uptake rate at midday in summer increased with leaf area index (LAI) across the studied forest ecosystems (Table 1 and Fig. S9). As F-RAN was selectively harvested (Sect. 2.3), the leaf area was decreased, which can result in a lower CO_2 uptake rate than in other forests under similar air temperature and PPFD conditions. Additionally, the peat soil at F-JAR and F-RAN can induce higher respiration (Fig. 2). Hence, even though the LAI and air temperature at F-JAR were, respectively, 23 % and 10 % higher than at F-HYY, the NEE at F-JAR was only 4 % lower than that at F-HYY. In the agricultural fields, the LAI and air temperature were comparable or higher than in the forests, which may explain the high momentary CO_2 uptake rate at midday during summer in the agricultural fields.

In the case of N_{neg}, the precursor of aerosol production largely influences N_{neg}. The trends of N_{neg} varying with air temperature and radiation were not evident (Figs. 9 and S9). H_2SO_4 formation can drive the nucleation process and is influenced by the sulfur dioxide concentration and radiation. As the garden area and agricultural fields in this study are located in or nearby cities, the SO_2 concentration there may be enhanced due to the anthropogenic pollution and its long-range transport. Also, the terpene emissions can initiate NPF, which has been observed in Siikaneva peatland and has led to stronger NPF there than that at F-HYY (Junninen et al., 2022; Huang et al., 2024). However, these events were reported to occur mostly in the late evening. Different plant species can emit different types of BVOCs (Guenther et al., 2012); e.g. monoterpenes are found to be dominant in coniferous forests, and isoprenes are dominant in broadleaf forests. The oxidation products of monoterpenes can enhance aerosol formation and growth (Rose et al., 2018), while isoprene has been reported to inhibit new particle formation (Kiendler-Scharr et al., 2009). As birch species are mixed with coniferous species at F-JAR, the possibly higher isoprene emission than in the other three predominantly coniferous forests may partially explain the lower N_{neg} at F-JAR. Moreover, the enhanced NH_3 in agricultural fields can play a synergistic role with both H_2SO_4 and low volatile organic compounds in clustering (Dada et al., 2023), which may explain the generally high N_{neg} in the three studied agricultural fields.

Overall, our results showed that agricultural fields have the highest potential to contribute to momentary CO_2 uptake and aerosol formation, affected by their vegetation and management practises. However, carbon inputs from fertilization and removal through harvested biomass in agricultural fields, which were not considered in our study, can lead to net carbon emissions in the annual carbon budgets (Heimsch et al., 2021, and references therein). Moreover, forests are the dominant landscape in Finland, covering ~ 9 times the area of agricultural fields (Table 2). Considering their large area, boreal forests in Finland are very likely to be the largest contributor to climate cooling when considering the CO_2 uptake and local new particle formation.

3.4 Research limitations

In our study, data covering only 1 year were applied to the stations with newly established atmospheric measurements, i.e. A-VII, although the measurements are continuing. The inter-annual variation in NEE has been widely observed across sites, e.g. F-HYY (Neefjes et al., 2022) and A-QVI (Heimsch et al., 2021), possibly due to annual changes in temperature and precipitation. In the reported year at A-VII, the air temperature was higher than that during 2015–2020 (Finnish Meteorological Institute, 2024; Fig. S8). Since a higher air temperature can simultaneously increase the respiration and photosynthesis in an ecosystem, the influence of increased air temperature on the net CO_2 flux, i.e. NEE, is

Table 2. Comparison of NEE and negative intermediate ions within the 2.0–2.3 nm size range across the hemi-boreal and boreal ecosystems at midday (10:00–14:00 LT) in summer. The errors for the median N_{neg} and NEE are the standard deviation of their values across all of the available years.

Ecosystem	Site (site ID)	Area in Finland (ha)	Median N_{neg} ($1\,cm^{-3}$)	Median N_{neg}/median $N_{neg,\,F\text{-}HYY}$	75th percentile N_{neg}/75th percentile $N_{neg,\,F\text{-}HYY}$	Midday NEE ($\mu mol\,m^{-2}\,s^{-1}$)	Median NEE/median $NEE_{F\text{-}HYY}$	25th percentile NEE/25th percentile $NEE_{F\text{-}HYY}$
Forest	Hyytiälä (F-HYY)	20.3×10^6 [a]	3.3 ± 0.53	1	1	-11.8 ± 1.3	1	1
	Värriö (F-VAR)		2.2 ± 0.13	0.67	0.87	-4.7 ± 1.2	0.4	0.52
	Järvselja (F-JAR)		1.7 ± 0.12	0.53	0.58	-12 ± 3.0	1.03	1.15
Drained-peatland forest	Ränskälänkorpi (F-RAN)	4.2×10^6 [a]	1.7 ± 0.18	0.53	0.57	-6.4 ± 2.3	0.54	0.61
Agricultural field	Haltiala (A-HAL)	2.3×10^6 [a]	2.7 ± 0.22	0.94	1.06	-10 ± 15	1.66	1.88
	Qvidja (A-QVI)		3.3 ± 0.30	1.01	1.17	-8.4 ± 3.9	0.71	0.86
	Viikki (A-VII)		2.9	0.88	0.97	−14	1.14	1.13
Open peatland	Siikaneva (P-SII)	0.21×10^6 [b]	2.5 ± 0.26	0.77	0.85	-3.6 ± 0.87	0.31	0.31
Urban garden area	Kumpula (G-KUM)	–	7.3 ± 0.68	2.24	2.86	-7.4 ± 2.2	0.63	0.73
Coastal area	Tvärminne (C-TVA)	–	1.2 ± 0.07	0.36	0.46	-0.01 ± 0.22	0.00	0.02

[a] Natural Resources Institute Finland (2022). [b] The area of oligotrophic open fens (Turunen and Valpola, 2020) – data not available.

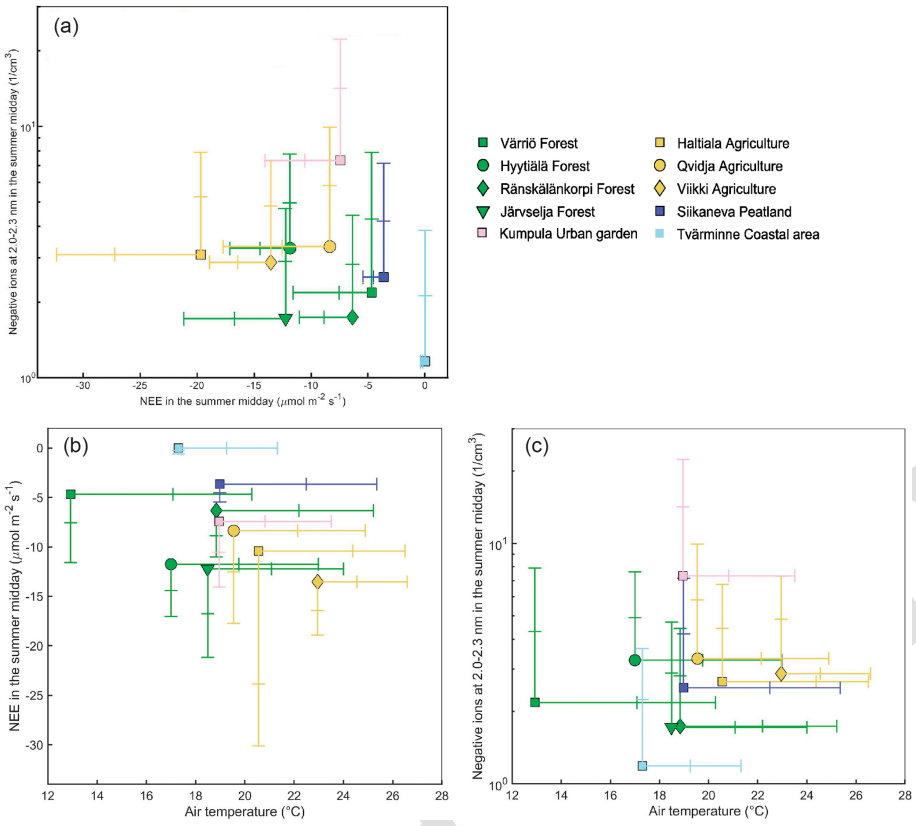

Figure 9. Comparison of net ecosystem exchange (NEE) and negative intermediate ions at 2.0–2.3 nm **(a)**, NEE and air temperature **(b)**, and negative intermediate ions at 2.0–2.3 nm and air temperature **(c)** across different sites. The dots represent median values at midday during summer (10:00–14:00 LT). Error bars indicate the 10th and 25th percentiles for NEE and the 75th and 90th percentiles for negative intermediate ions and air temperature, reflecting the CO_2 uptake rate and aerosol formation under optimal conditions.

quite site-specific. More observation years are needed to reduce the estimation errors of NEE. Compared with NEE, the inter-annul variation in N_{neg} at midday during summer fluctuated at a small magnitude across years (Table 2). Hence, the measured N_{neg} in the reported year can be considered to be relatively representative of the local aerosol production at the site. Moreover, the N_{neg} may originate from areas (sub-1 km; Tuovinen et al., 2024) larger than the ecosystem coverage, e.g. the agricultural sites within a radius of 500 m, leading to unavoidable uncertainties in the results.

Another potent greenhouse gas, methane (CH_4), can be emitted through microbial activities under anoxic conditions, e.g. peatlands and coastal areas (Mathijssen et al., 2022; Roth et al., 2023). Considering the fact that CH_4 has a sustained-flux global warming potential 45 times that of CO_2 over 100 years (Roth et al., 2023, and the reference therein), the net CO_2 equivalent emission of CH_4 is estimated to be 2.5–8.6 times that of CO_2 uptake at P-SII (Mathijssen et al., 2022). CH_4 emissions may largely compensate for the CO_2 uptake in open and non-ditched peatlands. Similarly, the emission of CH_4 from coastal environments around the Baltic Sea may offset 28 % of the CO_2 sink in macroalgae-dominated coastal areas (Roth et al., 2023). For ions, the summertime midday median N_{neg} at P-SII was 77 % of that at F-HYY (Table 2). As the open peatland is surrounded by forest within 1 km, the negative ion at 2.0–2.3 nm may be influenced by nearby forests.

Additionally, the albedo varies between each ecosystem type due to variations in vegetation cover (Peräkylä et al., 2025). Our research focused on the potential of different ecosystems for momentary CO_2 uptake and local aerosol production, thus omitting the albedo impact. Further research is still needed to evaluate the total climate impacts at the ecosystem level, including other greenhouse gas emissions and/or uptake, albedo, carbon input from fertilization (for agricultural fields), and biomass harvests.

4 Conclusions

The CarbonSink+ potential concept was established recently and provides a direct comparison of local contributions to CO_2 uptake and aerosol formation at the ecosystem scale. The value of negative intermediate ion concentrations within the 2.0–2.3 nm size range (N_{neg}) was applied as an indicator

of the corresponding contribution of each ecosystem to producing new aerosol particles which, after their subsequent growth to larger sizes, are able to cool the atmosphere at a regional scale. Following this concept, net ecosystem CO_2 exchange fluxes (NEE) and N_{neg} were analysed in 10 hemiboreal and boreal ecosystems in Finland and Estonia.

The results showed that the agricultural fields had similar or even 15 % higher CO_2 uptake potential compared to F-HYY during the summer at midday, possibly due to the high leaf area index and air temperature in the agricultural fields. A distinct CO_2 uptake in the urban garden at midday in summer was observed, resulting from the strong photosynthesis of vegetation within the site. The uptake rate was 37 % lower than that at F-HYY but ∼ 2 times of that in the open peatland. The coastal area considered in this study remained a very small CO_2 sink during summertime. The differences in N_{neg} between the studied sites were not as large as those in NEE. Ubiquitous nighttime clustering was observed across the terrestrial ecosystems. At midday in summer, N_{neg} was highest in the urban garden, followed by the agricultural fields. The coastal area had the lowest N_{neg}. The forest sites generally had lower N_{neg} than the agricultural sites. In agricultural fields, the synergetic role of NH_3, H_2SO_4, and low volatile organic compounds originating from BVOC oxidation may generally play a synergistic role in clustering and induce a high N_{neg} when compared with other ecosystem types. The N_{neg} in the open peatland was 23 % lower than that at F-HYY but 14 %–46 % higher than that at other studied forests. Note that the urban garden and agricultural sites in Helsinki might be more influenced by air pollution compared to the forests and open peatland that were receiving little anthropogenic interference and pollution. The agricultural fields present the highest potential to contribute to momentary CO_2 uptake and aerosol formation. However, it should be noted that the carbon in fertilization inputs and harvested biomass in agricultural fields were not included in this study. Overall, considering the large area of forests in Finland and Estonia, the forests, in total, are the largest contributors to climate cooling in terms of their CO_2 uptake and local new particle formation.

Data availability. Measurement data from the sites, including ion data, eddy covariance data, and meteorological data, will be available upon request from the corresponding author before the relevant databases are made open to the public.

Supplement. The supplement related to this article is available online at [the link will be implemented upon publication].

Author contributions. ST, JL, and RT were responsible for the ion measurements. PS, AL, MP, AL, MK, HR, LH, AV, IM, and SN were responsible for the eddy covariance measurements and analysed the raw data. MK designed the study. PKe, AL, PKo, TN, OP, EE, TK, JB, VMK, and MK analysed the data and interpreted the results. PKe prepared the first draft of the paper. All of the authors contributed to the discussion of the results and provided input for the paper.

Competing interests. The contact author has declared that none of the authors has any competing interests.

Disclaimer. Publisher's note: Copernicus Publications remains neutral with regard to jurisdictional claims made in the text, published maps, institutional affiliations, or any other geographical representation in this paper. While Copernicus Publications makes every effort to include appropriate place names, the final responsibility lies with the authors.

Acknowledgements. We express our gratitude to the technical and scientific staff at all measurement sites for their invaluable contributions. We also acknowledge institutional support from the following projects and infrastructures: the ACCC Flagship initiative funded by the Academy of Finland; the Academy Professorship programme; the Strategic Research Council; the "Gigacity" project sponsored by the Jenny and Antti Wihuri Foundation; the European Research Council (ERC) ATM-GTP initiative; the FOCI consortium (Non-CO2 Forcers and their Climate, Weather, Air Quality and Health Impacts); the University of Helsinki's ACTRIS-HY framework; SMEAR Estonia; and the INAR RI, ICOS RI, ACTRIS RI, and eLTER RI research infrastructures.

Financial support. This work has been supported by the Academy of Finland through grant nos. 337549, 337552, 302958, 1325656, 311932, 334792, 316114, 325647, 325681, 339489, 352431, and 347782; the European Union via the NextGenerationEU instrument (grant no. PRG 347782), the EU Horizon 2020 Research and Innovation programme (grant agreement no. 871115 for ACTRIS IMP), the ERC Advanced Grant ATM-GTP 742206, and the FOCI initiative; the Estonian Research Council (grant no. 1674); the Estonian Environmental Investment Centre (project no. 18392); and philanthropic foundations including the Jenny and Antti Wihuri Foundation and the Jane and Aatos Erkko Foundation.

Open-access funding was provided by the Helsinki University Library.

Review statement. This paper was edited by Akihiko Ito and reviewed by two anonymous referees.

References

Aalto, J., Anttila, V., Kolari, P., Korpela, I., Isotalo, A., Levula, J., Schiestl-Aalto, P., and Bäck, J.: Hyytiälä SMEAR II Forest year

2020 thinning tree and carbon inventory data, Zenodo [data set], https://doi.org/10.5281/zenodo.7639833, 2023.

Alekseychik, P., Korrensalo, A., Mammarella, I., Launiainen, S., Tuittila, E.-S., Korpela, I., and Vesala, T.: Carbon balance of a Finnish bog: temporal variability and limiting factors based on 6 years of eddy-covariance data, Biogeosciences, 18, 4681–4704, https://doi.org/10.5194/bg-18-4681-2021, 2021.

Aliaga, D., Tuovinen, S., Zhang, T., Lampilahti, J., Li, X., Ahonen, L., Kokkonen, T., Nieminen, T., Hakala, S., Paasonen, P., Bianchi, F., Worsnop, D., Kerminen, V.-M., and Kulmala, M.: Nanoparticle ranking analysis: determining new particle formation (NPF) event occurrence and intensity based on the concentration spectrum of formed (sub-5 nm) particles, Aerosol Research, 1, 81–92, https://doi.org/10.5194/ar-1-81-2023, 2023.

Artaxo, P., Hansson, H.-C., Andreae, M. O., Bäck, J., Alves, E. G., Barbosa, H. M. J., Bender, F., Bourtsoukidis, E., Carbone, S., Chi, J., Decesari, S., Després, V. R., Ditas, F., Ezhova, E., Fuzzi, S., Hasselquist, N. J., Heintzenberg, J., Holanda, B. A., Guenther, A., Hakola, H., Heikkinen, L., Kerminen, V.-M., Kontkanen, J., Krejci, R., Kulmala, M., Lavric, J. V., De Leeuw, G., Lehtipalo, K., Machado, L. A. T., McFiggans, G., Franco, M. A. M., Meller, B. B., Morais, F. G., Mohr, C., Morgan, W., Nilsson, M. B., Peichl, M., Petäjä, T., Praß, M., Pöhlker, C., Pöhlker, M. L., Pöschl, U., Von Randow, C., Riipinen, I., Rinne, J., Rizzo, L. V., Rosenfeld, D., Silva Dias, M. A. F., Sogacheva, L., Stier, P., Swietlicki, E., Sörgel, M., Tunved, P., Virkkula, A., Wang, J., Weber, B., Yáñez-Serrano, A. M., Zieger, P., Mikhailov, E., Smith, J. N., and Kesselmeier, J.: Tropical and Boreal Forest – Atmosphere Interactions: A Review, Tellus B, 74, 24–162, https://doi.org/10.16993/tellusb.34, 2022.

Aubinet, M., Grelle, A., Ibrom, A., Rannik, Ü., Moncrieff, J., Foken, T., Kowalski, A. S., Martin, P. H., Berbigier, P., Bernhofer, C., Clement, R., Elbers, J., Granier, A., Grünwald, T., Morgenstern, K., Pilegaard, K., Rebmann, C., Snijders, W., Valentini, R., and Vesala, T.: Estimates of the Annual Net Carbon and Water Exchange of Forests: The EUROFLUX Methodology, in: Advances in Ecological Research, edited by: Fitter, A. H. and Raffaelli, D. G., Academic Press, 113–175, https://doi.org/10.1016/S0065-2504(08)60018-5, 1999.

Chang, J. F., Ciais, P., Gasser, T., Smith, P., Herrero, M., Havlik, P., Obersteiner, M., Guenet, B., Goll, D. S., Li, W., Naipal, V., Peng, S. S., Qiu, C. J., Tian, H. Q., Viovy, N., Yue, C., and Zhu, D.: Climate warming from managed grasslands cancels the cooling effect of carbon sinks in sparsely grazed and natural grasslands, Nat. Commun., 12, 118, https://doi.org/10.1038/s41467-020-20406-7, 2021.

Chen, X., Kerminen, V.-M., Paatero, J., Paasonen, P., Manninen, H. E., Nieminen, T., Petäjä, T., and Kulmala, M.: How do air ions reflect variations in ionising radiation in the lower atmosphere in a boreal forest?, Atmos. Chem. Phys., 16, 14297–14315, https://doi.org/10.5194/acp-16-14297-2016, 2016.

Copernicus Global Land Service: Land Cover 2018 (raster 100 m), global, yearly – version 3, https://land.copernicus.eu/en/products/global-dynamic-land-cover/copernicus-global-land-service-land-cover-100m-collection-3-epoch-2018-globe (last access: 13 July 2023), 2020.

Dada, L., Chellapermal, R., Buenrostro Mazon, S., Paasonen, P., Lampilahti, J., Manninen, H. E., Junninen, H., Petäjä, T., Kerminen, V.-M., and Kulmala, M.: Refined classification and characterization of atmospheric new-particle formation events using air ions, Atmos. Chem. Phys., 18, 17883–17893, https://doi.org/10.5194/acp-18-17883-2018, 2018.

Dada, L., Okuljar, M., Shen, J., Olin, M., Heimsch, L., Wu, Y., Baalbaki, R., Lampimäki, M., Kankaanrinta, S., Herlin, I., Kalliokoski, J., Lohila, A., Petäjä, T., Dal Maso, M., Duplissy, J., Kerminen, V.-M., and Kulmala, M.: Synergistic role of sulfuric acid, ammonia and organics in particle formation over an agricultural land, Environ. Sci. Atmos., 3, 1195–1211, https://doi.org/10.1039/d3ea00065f, 2023.

Ezhova, E., Ylivinkka, I., Kuusk, J., Komsaare, K., Vana, M., Krasnova, A., Noe, S., Arshinov, M., Belan, B., Park, S.-B., Lavrič, J. V., Heimann, M., Petäjä, T., Vesala, T., Mammarella, I., Kolari, P., Bäck, J., Rannik, Ü., Kerminen, V.-M., and Kulmala, M.: Direct effect of aerosols on solar radiation and gross primary production in boreal and hemiboreal forests, Atmos. Chem. Phys., 18, 17863–17881, https://doi.org/10.5194/acp-18-17863-2018, 2018.

Finnish Meteorological Institute: Download observations, https://en.ilmatieteenlaitos.fi/download-observations (last access: 26 February 2024), 2024.

Foken, T. and Wichura, B.: Tools for quality assessment of surface-based flux measurements, Agric. For. Meteorol., 78, 83–105, https://doi.org/10.1016/0168-1923(95)02248-1, 1996.

Fratini, G. and Mauder, M.: Towards a consistent eddy-covariance processing: an intercomparison of EddyPro and TK3, Atmos. Meas. Tech., 7, 2273–2281, https://doi.org/10.5194/amt-7-2273-2014, 2014.

Friedlingstein, P., O'Sullivan, M., Jones, M. W., Andrew, R. M., Gregor, L., Hauck, J., Le Quéré, C., Luijkx, I. T., Olsen, A., Peters, G. P., Peters, W., Pongratz, J., Schwingshackl, C., Sitch, S., Canadell, J. G., Ciais, P., Jackson, R. B., Alin, S. R., Alkama, R., Arneth, A., Arora, V. K., Bates, N. R., Becker, M., Bellouin, N., Bittig, H. C., Bopp, L., Chevallier, F., Chini, L. P., Cronin, M., Evans, W., Falk, S., Feely, R. A., Gasser, T., Gehlen, M., Gkritzalis, T., Gloege, L., Grassi, G., Gruber, N., Gürses, Ö., Harris, I., Hefner, M., Houghton, R. A., Hurtt, G. C., Iida, Y., Ilyina, T., Jain, A. K., Jersild, A., Kadono, K., Kato, E., Kennedy, D., Klein Goldewijk, K., Knauer, J., Korsbakken, J. I., Landschützer, P., Lefèvre, N., Lindsay, K., Liu, J., Liu, Z., Marland, G., Mayot, N., McGrath, M. J., Metzl, N., Monacci, N. M., Munro, D. R., Nakaoka, S.-I., Niwa, Y., O'Brien, K., Ono, T., Palmer, P. I., Pan, N., Pierrot, D., Pocock, K., Poulter, B., Resplandy, L., Robertson, E., Rödenbeck, C., Rodriguez, C., Rosan, T. M., Schwinger, J., Séférian, R., Shutler, J. D., Skjelvan, I., Steinhoff, T., Sun, Q., Sutton, A. J., Sweeney, C., Takao, S., Tanhua, T., Tans, P. P., Tian, X., Tian, H., Tilbrook, B., Tsujino, H., Tubiello, F., van der Werf, G. R., Walker, A. P., Wanninkhof, R., Whitehead, C., Willstrand Wranne, A., Wright, R., Yuan, W., Yue, C., Yue, X., Zaehle, S., Zeng, J., and Zheng, B.: Global Carbon Budget 2022, Earth Syst. Sci. Data, 14, 4811–4900, https://doi.org/10.5194/essd-14-4811-2022, 2022.

Gordon, H., Kirkby, J., Baltensperger, U., Bianchi, F., Breitenlechner, M., Curtius, J., Dias, A., Dommen, J., Donahue, N. M., Dunne, E. M., Duplissy, J., Ehrhart, S., Flagan, R. C., Frege, C., Fuchs, C., Hansel, A., Hoyle, C. R., Kulmala, M., Kürten, A., Lehtipalo, K., Makhmutov, V., Molteni, U., Rissanen, M. P., Stozkhov, Y., Tröstl, J., Tsagkogeor-

gas, G., Wagner, R., Williamson, C., Wimmer, D., Winkler, P. M., Yan, C., and Carslaw, K. S.: Causes and importance of new particle formation in the present-day and preindustrial atmospheres, J. Geophys. Res.-Atmos., 122, 8739–8760, https://doi.org/10.1002/2017JD026844, 2017.

Guenther, A. B., Jiang, X., Heald, C. L., Sakulyanontvittaya, T., Duhl, T., Emmons, L. K., and Wang, X.: The Model of Emissions of Gases and Aerosols from Nature version 2.1 (MEGAN2.1): an extended and updated framework for modeling biogenic emissions, Geosci. Model Dev., 5, 1471–1492, https://doi.org/10.5194/gmd-5-1471-2012, 2012.

Hari, P. and Kulmala, M.: Station for Measuring Ecosystem-At mosphere Relations (SMEAR II), Boreal Environ. Res., 10, 315–322, 2005.

Heimsch, L., Lohila, A., Tuovinen, J.-P., Vekuri, H., Heinonsalo, J., Nevalainen, O., Korkiakoski, M., Liski, J., Laurila, T., and Kulmala, L.: Carbon dioxide fluxes and carbon balance of an agricultural grassland in southern Finland, Biogeosciences, 18, 3467–3483, https://doi.org/10.5194/bg-18-3467-2021, 2021.

Huang, W., Junninen, H., Garmash, O., Lehtipalo, K., Stolzenburg, D., Lampilahti, J., Ezhova, E., Schallhart, S., Rantala, P., Aliaga, D., Ahonen, L., Sulo, J., Quéléver, L. L. J., Cai, R., Alekseychik, P., Mazon, S. B., Yao, L., M. Blichner, S., Zha, Q., Mammarella, I., Kirkby, J., Kerminen, V.-M., Worsnop, D. R., Kulmala, M., and Bianchi, F.: Potential pre-industrial-like new particle formation induced by pure biogenic organic vapors in Finnish peatland, Sci. Adv., 10, eadm9191, https://doi.org/10.1126/sciadv.adm9191,2024.

IPCC: Annex I: Glossary, in: Global Warming of 1.5 °C: IPCC Special Report on Impacts of Global Warming of 1.5 °C above Pre-industrial Levels in Context of Strengthening Response to Climate Change, Sustainable Development, and Efforts to Eradicate Poverty, edited by: Intergovernmental Panel on Climate, C., Cambridge University Press, Cambridge, 541–562, https://doi.org/10.1017/9781009157940.008, 2022.

Järvi, L., Nordbo, A., Junninen, H., Riikonen, A., Moilanen, J., Nikinmaa, E., and Vesala, T.: Seasonal and annual variation of carbon dioxide surface fluxes in Helsinki, Finland, in 2006–2010, Atmos. Chem. Phys., 12, 8475–8489, https://doi.org/10.5194/acp-12-8475-2012, 2012.

Jia, G., Shevliakova, E., Artaxo, P., Noblet-Ducoudré, N. D., Houghton, R., House, J., Kitajima, K., Lennard, C., Popp, A., Sirin, A., Sukumar, R., and Verchot, L. Land–Climate interactions. In: Climate Change and Land: An IPCC Special Report on Climate Change, Desertification, Land Degradation, Sustainable Land Management, Food Security, and Greenhouse Gas Fluxes in Terrestrial Ecosystems, edited by: Shukla, P. R., Skea, J., Calvo Buendia, E., Masson-Delmotte, V., Pörtner, H.-O., Roberts, D. C., Zhai, P., Slade, R., Connors, S., van Diemen, R., Ferrat, M., Haughey, E., Luz, S., Neogi, S., Pathak, M., Petzold, J., Portugal Pereira, J., Vyas, P., Huntley, E., Kissick, K., Belkacemi, M., and Malley, J., Cambridge University Press, Cambridge, 131–248, https://doi.org/10.1017/9781009157988.004, 2022.

Junninen, H., Ahonen, L., Bianchi, F., Quéléver, L., Schallhart, S., Dada, L., Manninen, H. E., Leino, K., Lampilahti, J., Buenrostro Mazon, S., Rantala, P., Räty, M., Kontkanen, J., Negri, S., Aliaga, D., Garmash, O., Alekseychik, P., Lipp, H., Tamme, K., Levula, J., Sipilä, M., Ehn, M., Worsnop, D., Zilitinkevich, S., Mammarella, I., Rinne, J., Vesala, T., Petäjä, T., Kerminen, V.-M., and Kulmala, M.: Terpene emissions from boreal wetlands can initiate stronger atmospheric new particle formation than boreal forests, Commun. Earth Environ., 3, 93, https://doi.org/10.1038/s43247-022-00406-9, 2022.

Kammer, J., Simon, L., Ciuraru, R., Petit, J.-E., Lafouge, F., Buysse, P., Bsaibes, S., Henderson, B., Cristescu, S. M., Durand, B., Fanucci, O., Truong, F., Gros, V., and Loubet, B.: New particle formation at a peri-urban agricultural site, Sci. Total Environ., 857, 159370, https://doi.org/10.1016/j.scitotenv.2022.159370, 2023.

Kangur, A., Nigul, K., Padari, A., Kiviste, A., Korjus, H., Laarmann, D., Põldveer, E., Mitt, R., Frelich, L., Jõgiste, K., Stanturf, J., Paluots, T., Kängsepp, V., Jürgenson, H., Noe, S., Sims, A., and Metslaid, M.: Composition of live, dead and downed trees in Järvselja old-growth forest, Forestry Studies/Metsanduslikud Uurimused, 75, 15–40, https://doi.org/10.2478/fsmu-2021-0009, 2021.

Kerminen, V.-M., Chen, X., Vakkari, V., Petäjä, T., Kulmala, M., and Bianchi, F.: Atmospheric new particle formation and growth: review of field observations, Environ. Res. Lett., 13, 103003, https://doi.org/10.1088/1748-9326/aadf3c, 2018.

Kiendler-Scharr, A., Wildt, J., Maso, M. D., Hohaus, T., Kleist, E., Mentel, T. F., Tillmann, R., Uerlings, R., Schurr, U., and Wahner, A.: New particle formation in forests inhibited by isoprene emissions, Nature, 461, 381–384, https://doi.org/10.1038/nature08292, 2009.

Kulmala, M., Ezhova, E., Kalliokoski, T., Noe, S., Vesala, T., Lohila, A., Liski, J., Makkonen, R., Bäck, J., Petäjä, T., Kerminen, V.-M., and Kerminen, P.: CarbonSink+ – Accounting for multiple climate feedbacks from forests, Boreal Environ. Res., 25, 145–159, 2020.

Kulmala, M., Ke, P., Lintunen, A., Peräkylä, O., Lohtander, A., Tuovinen, S., Lampilahti, J., Kolari, P., Schiestl-Aalto, P., Kokkonen, T., Nieminen, T., Dada, L., Ylivinkka, I., Petäjä, T., Bäck, J., Lohila, A., Heimsch, L., Ezhova, E., and Kerminen, V.-M.: A novel concept for assessing the potential of different boreal ecosystems to mitigate climate change (CarbonSink+ Potential), Boreal Environ. Res., 29, 1–16, 2024.

Mäki, M., Ryhti, K., Fer, I., Ťupek, B., Vestin, P., Roland, M., Lehner, I., Köster, E., Lehtonen, A., Bäck, J., Heinonsalo, J., Pumpanen, J., and Kulmala, L.: Heterotrophic and rhizospheric respiration in coniferous forest soils along a latitudinal gradient, Agr. Forest Meteorol., 317, 108876, https://doi.org/10.1016/j.agrformet.2022.108876, 2022.

Kulmala, L., Pumpanen, J., Kolari, P., Dengel, S., Berninger, F., Köster, K., Matkala, L., Vanhatalo, A., Vesala, T., and Bäck, J.: Inter- and intra-annual dynamics of photosynthesis differ between forest floor vegetation and tree canopy in a subarctic Scots pine stand, Agric. For. Meteorol., 271, 1–11, https://doi.org/10.1016/j.agrformet.2019.02.029, 2019.

Kulmala, M., Suni, T., Lehtinen, K. E. J., Dal Maso, M., Boy, M., Reissell, A., Rannik, Ü., Aalto, P., Keronen, P., Hakola, H., Bäck, J., Hoffmann, T., Vesala, T., and Hari, P.: A new feedback mechanism linking forests, aerosols, and climate, Atmos. Chem. Phys., 4, 557–562, https://doi.org/10.5194/acp-4-557-2004, 2004.

Kulmala, M., Nieminen, T., Nikandrova, A., Lehtipalo, K., Manninen, H., Kajos, M., Kolari, P., Lauri, A., Petaja, T., Krejci, R., Hansson, H.-C., Swietlicki, E., Lindroth, A., Christensen, T. R.,

Arneth, A., Hari, P., Back, J., Vesala, T., and Kerminen, V.-M.: CO_2-induced terrestrial climate feedback mechanism: from carbon sink to aerosol source and back, Boreal Environ. Res., 19, 122–131, 2014.

Laurila, T., Aurela, M., Hatakka, J., Hotanen, J.-P., Jauhiainen, J., Korkiakoski, M., Korpela, L., Koskinen, M., Laiho, R., Lehtonen, A., Alder, K., Linkosalmi, M., Salmon, A., Minkkinen, K., Mäkelä, T., Mäkiranta, P., Nieminen, M., Ojanen, P., Peltoniemi, M., Penttilä, T., Rainne, J., Rautakoski, H., Saarinen, M., Salovaara, P., Sarkkola, S., and Mäkipää, R. : Set-up and instrumentation of the greenhouse gas (GHG) measurements on experimental sites of continuous cover forestry, Natural Resources and Bioeconomy Studies, 26, 1–53, 2021.

Lee, X. and Hu, X.: Forest-air fluxes of carbon, water and energy over non-flat terrain, Bound.-Layer Meteorol., 103, 277–301, https://doi.org/10.1023/A:1014508928693, 2002.

Mammarella, I., Peltola, O., Nordbo, A., Järvi, L., and Rannik, Ü.: Quantifying the uncertainty of eddy covariance fluxes due to the use of different software packages and combinations of processing steps in two contrasting ecosystems, Atmos. Meas. Tech., 9, 4915–4933, https://doi.org/10.5194/amt-9-4915-2016, 2016.

Manninen, H. E., Mirme, S., Mirme, A., Petäjä, T., and Kulmala, M.: How to reliably detect molecular clusters and nucleation mode particles with Neutral cluster and Air Ion Spectrometer (NAIS), Atmos. Meas. Tech., 9, 3577–3605, https://doi.org/10.5194/amt-9-3577-2016, 2016.

Mathijssen, P. J. H., Tuovinen, J. P., Lohila, A., Väliranta, M., and Tuittila, E. S.: Identifying main uncertainties in estimating past and present radiative forcing of peatlands, Glob. Change Biol., 28, 4069–4084, https://doi.org/10.1111/gcb.16189, 2022.

Mazon, S. B., Kontkanen, J., Manninen, H. E., Nieminen, T., Kerminen, V. M., and Kulmala, M.: A long-term comparison of nighttime cluster events and daytime ion formation in a boreal forest, Boreal Environ. Res., 21, 242–261, 2016.

Mirme, S. and Mirme, A.: The mathematical principles and design of the NAIS – a spectrometer for the measurement of cluster ion and nanometer aerosol size distributions, Atmos. Meas. Tech., 6, 1061–1071, https://doi.org/10.5194/amt-6-1061-2013, 2013.

Natural Resources Institute Finland: Natural Resources Data Service, https://www.luke.fi/en/statistics (last access: 25 July 2023), 2022.

Neefjes, I., Laapas, M., Médus, E., Meittunen, E., Ahonen, L., Quéléver, L., Aaltio, J., Bäck, J., Kerminen, V.-M., Lampilahti, J., Luoma, K., Maki, M., Marmmarella, I., Petäjä, T., Räty, M., Sarnela, N., Ylivinkka, I., Hakala, S., Kulmala, M., and Liu, Y.: 25 years of atmospheric and ecosystem measurements in a boreal forest – Seasonal variation and responses to warm and dry years, Boreal Environ. Res., 27, 1–31, 2022.

Nieminen, T., Kerminen, V.-M., Petäjä, T., Aalto, P. P., Arshinov, M., Asmi, E., Baltensperger, U., Beddows, D. C. S., Beukes, J. P., Collins, D., Ding, A., Harrison, R. M., Henzing, B., Hooda, R., Hu, M., Hõrrak, U., Kivekäs, N., Komsaare, K., Krejci, R., Kristensson, A., Laakso, L., Laaksonen, A., Leaitch, W. R., Lihavainen, H., Mihalopoulos, N., Németh, Z., Nie, W., O'Dowd, C., Salma, I., Sellegri, K., Svenningsson, B., Swietlicki, E., Tunved, P., Ulevicius, V., Vakkari, V., Vana, M., Wiedensohler, A., Wu, Z., Virtanen, A., and Kulmala, M.: Global analysis of continental boundary layer new particle formation based on long-term measurements, Atmos. Chem. Phys., 18, 14737–14756, https://doi.org/10.5194/acp-18-14737-2018, 2018.

Noe, S., Niinemets, Ü., Krasnova, A., Krasnov, D., Motallebi, A., Kängsepp, V., Jõgiste, K., Hõrrak, U., Komsaare, K., Mirme, S., Vana, M., Tammet, H., Bäck, J., Vesala, T., Kulmala, M., Petäjä, T., and Kangur, A.: SMEAR Estonia: Perspectives of a large-scale forest ecosystem– Atmosphere research infrastructure, For. Stud., 63, 56–84, https://doi.org/10.1515/fsmu-2015-0009, 2015.

Olin, M., Okuljar, M., Rissanen, M. P., Kalliokoski, J., Shen, J., Dada, L., Lampimäki, M., Wu, Y., Lohila, A., Duplissy, J., Sipilä, M., Petäjä, T., Kulmala, M., and Dal Maso, M.: Measurement report: Atmospheric new particle formation in a coastal agricultural site explained with binPMF analysis of nitrate CI-APi-TOF spectra, Atmos. Chem. Phys., 22, 8097–8115, https://doi.org/10.5194/acp-22-8097-2022, 2022.

Peräkylä, O., Rinne, E., Ezhova, E., Lintunen, A., Lohila, A., Aalto, J., Aurela, M., Kolari, P., and Kulmala, M.: Comparison of shortwave radiation dynamics between boreal forest and open peatland pairs in southern and northern Finland, Biogeosciences, 22, 153–179, https://doi.org/10.5194/bg-22-153-2025, 2025.

Petäjä, T., Tabakova, K., Manninen, A., Ezhova, E., O'Connor, E., Moisseev, D., Sinclair, V. A., Backman, J., Levula, J., Luoma, K., Virkkula, A., Paramonov, M., Räty, M., Äijälä, M., Heikkinen, L., Ehn, M., Sipilä, M., Yli-Juuti, T., Virtanen, A., Ritsche, M., Hickmon, N., Pulik, G., Rosenfeld, D., Worsnop, D. R., Bäck, J., Kulmala, M., and Kerminen, V. M.: Influence of biogenic emissions from boreal forests on aerosol–cloud interactions, Nat. Geosci., 15, 42–47, https://doi.org/10.1038/s41561-021-00876-0, 2022.

Räty, M., Sogacheva, L., Keskinen, H.-M., Kerminen, V.-M., Nieminen, T., Petäjä, T., Ezhova, E., and Kulmala, M.: Dynamics of aerosol, humidity, and clouds in air masses travelling over Fennoscandian boreal forests, Atmos. Chem. Phys., 23, 3779–3798, https://doi.org/10.5194/acp-23-3779-2023, 2023.

Regnier, P., Resplandy, L., Najjar, R. G., and Ciais, P.: The land-to-ocean loops of the global carbon cycle, Nature, 603, 401–410, https://doi.org/10.1038/s41586-021-04339-9, 2022.

Ren, J., Chen, L., Fan, T., Liu, J., Jiang, S., and Zhang, F.: The NPF effect on CCN number concentrations: A review and re-evaluation of observations from 35 sites worldwide, Geophys. Res. Lett., 48, e2021GL095190, https://doi.org/10.1029/2021GL095190, 2021.

Rinne, J., Tuittila, E.-S., Peltola, O., Li, X., Raivonen, M., Alekseychik, P., Haapanala, S., Pihlatie, M., Aurela, M., Mammarella, I., and Vesala, T.: Temporal Variation of Ecosystem Scale Methane Emission From a Boreal Fen in Relation to Temperature, Water Table Position, and Carbon Dioxide Fluxes, Global Biogeochem Cy., 32, 1087–1106, https://doi.org/10.1029/2017gb005747, 2018.

Rose, C., Zha, Q., Dada, L., Yan, C., Lehtipalo, K., Junninen, H., Mazon, S. B., Jokinen, T., Sarnela, N., Sipilä, M., Petäjä, T., Kerminen, V.-M., Bianchi, F., and Kulmala, M.: Observations of biogenic ion-induced cluster formation in the atmosphere, Science Advances, 4, eaar5218, https://doi.org/10.1126/sciadv.aar5218, 2018.

Rosenfeld, D., Andreae, M. O., Asmi, A., Chin, M., De Leeuw, G., Donovan, D. P., Kahn, R., Kinne, S., Kivekäs, N., Kulmala, M., Lau, W., Schmidt, K. S., Suni, T., Wagner, T., Wild, M., and Quaas, J.: Global observations of aerosol-cloud-

precipitation-climate interactions, Rev. Geophys., 52, 750–808, https://doi.org/10.1002/2013rg000441, 2014.

Roth, F., Broman, E., Sun, X., Bonaglia, S., Nascimento, F., Prytherch, J., Brüchert, V., Lundevall Zara, M., Brunberg, M., Geibel, M. C., Humborg, C., and Norkko, A.: Methane emissions offset atmospheric carbon dioxide uptake in coastal macroalgae, mixed vegetation and sediment ecosystems, Nat. Commun., 14, 42, https://doi.org/10.1038/s41467-022-35673-9, 2023.

Stolzenburg, D., Cai, R., Blichner, S. M., Kontkanen, J., Zhou, P., Makkonen, R., Kerminen, V.-M., Kulmala, M., Riipinen, I., and Kangasluoma, J.: Atmospheric nanoparticle growth, Rev. Mod. Phys., 95, 045002, https://doi.org/10.1103/RevModPhys.95.045002, 2023.

Tammet, H., Komsaare, K., and Hõrrak, U.: Intermediate ions in the atmosphere, Atmos. Res., 135–136, 263–273, https://doi.org/10.1016/j.atmosres.2012.09.009, 2014.

Turunen, J. and Valpola, S.: The influence of anthropogenic land use on Finnish peatland area and carbon stores 1950–2015, Mires and Peat, 1–27, https://doi.org/10.19189/MaP.2019.GDC.StA.1870, 2020.

Virtasalo, J. J., Österholm, P., and Asmala, E.: Estuarine flocculation dynamics of organic carbon and metals from boreal acid sulfate soils, Biogeosciences, 20, 2883–2901, https://doi.org/10.5194/bg-20-2883-2023, 2023.

Tuovinen, S., Lampilahti, J., Kerminen, V.-M., and Kulmala, M.: Intermediate ions as indicator for local new particle formation, Aerosol Research, 2, 93–105, https://doi.org/10.5194/ar-2-93-2024, 2024.

Walker, A. P., De Kauwe, M. G., Bastos, A., Belmecheri, S., Georgiou, K., Keeling, R. F., McMahon, S. M., Medlyn, B. E., Moore, D. J. P., Norby, R. J., Zaehle, S., Anderson-Teixeira, K. J., Battipaglia, G., Brienen, R. J. W., Cabugao, K. G., Cailleret, M., Campbell, E., Canadell, J. G., Ciais, P., Craig, M. E., Ellsworth, D. S., Farquhar, G. D., Fatichi, S., Fisher, J. B., Frank, D. C., Graven, H., Gu, L., Haverd, V., Heilman, K., Heimann, M., Hungate, B. A., Iversen, C. M., Joos, F., Jiang, M., Keenan, T. F., Knauer, J., Körner, C., Leshyk, V. O., Leuzinger, S., Liu, Y., Macbean, N., Malhi, Y., McVicar, T. R., Penuelas, J., Pongratz, J., Powell, A. S., Riutta, T., Sabot, M. E. B., Schleucher, J., Sitch, S., Smith, W. K., Sulman, B., Taylor, B., Terrer, C., Torn, M. S., Treseder, K. K., Trugman, A. T., Trumbore, S. E., Van Mantgem, P. J., Voelker, S. L., Whelan, M. E., and Zuidema, P. A.: Integrating the evidence for a terrestrial carbon sink caused by increasing atmospheric CO_2, New Phytol., 229, 2413–2445, https://doi.org/10.1111/nph.16866, 2021.

Yi, C. X., Ricciuto, D., Li, R., Wolbeck, J., Xu, X. Y., Nilsson, M., Aires, L., Albertson, J. D., Ammann, C., Arain, M. A., de Araujo, A. C., Aubinet, M., Aurela, M., Barcza, Z., Barr, A., Berbigier, P., Beringer, J., Bernhofer, C., Black, A. T., Bolstad, P. V., Bosveld, F. C., Broadmeadow, M. S. J., Buchmann, N., Burns, S. P., Cellier, P., Chen, J. M., Chen, J. Q., Ciais, P., Clement, R., Cook, B. D., Curtis, P. S., Dail, D. B., Dellwik, E., Delpierre, N., Desai, A. R., Dore, S., Dragoni, D., Drake, B. G., Dufrene, E., Dunn, A., Elbers, J., Eugster, W., Falk, M., Feigenwinter, C., Flanagan, L. B., Foken, T., Frank, J., Fuhrer, J., Gianelle, D., Goldstein, A., Goulden, M., Granier, A., Grünwald, T., Gu, L., Guo, H. Q., Hammerle, A., Han, S. J., Hanan, N. P., Haszpra, L., Heinesch, B., Helfter, C., Hendriks, D., Hutley, L. B., Ibrom, A., Jacobs, C., Johansson, T., Jongen, M., Katul, G., Kiely, G., Klumpp, K., Knohl, A., Kolb, T., Kutsch, W. L., Lafleur, P., Laurila, T., Leuning, R., Lindroth, A., Liu, H. P., Loubet, B., Manca, G., Marek, M., Margolis, H. A., Martin, T. A., Massman, W. J., Matamala, R., Matteucci, G., McCaughey, H., Merbold, L., Meyers, T., Migliavacca, M., Miglietta, F., Misson, L., Moelder, M., Moncrieff, J., Monson, R. K., Montagnani, L., Montes-Helu, M., Moors, E., Moureaux, C., Mukelabai, M. M., Munger, J. W., Myklebust, M., Nagy, Z., Noormets, A., Oechel, W., Oren, R., Pallardy, S. G., Kyaw, T. P. U., Pereira, J. S., Pilegaard, K., Pintér, K., Pio, C., Pita, G., Powell, T. L., Rambal, S., Randerson, J. T., von Randow, C., Rebmann, C., Rinne, J., Rossi, F., Roulet, N., Ryel, R. J., Sagerfors, J., Saigusa, N., Sanz, M. J., Mugnozza, G. S., Schmid, H. P., Seufert, G., Siqueira, M., Soussana, J. F., Starr, G., Sutton, M. A., Tenhunen, J., Tuba, Z., Tuovinen, J. P., Valentini, R., Vogel, C. S., Wang, J. X., Wang, S. Q., Wang, W. G., Welp, L. R., Wen, X. F., Wharton, S., Wilkinson, M., Williams, C. A., Wohlfahrt, G., Yamamoto, S., Yu, G. R., Zampedri, R., Zhao, B., and Zhao, X. Q.: Climate control of terrestrial carbon exchange across biomes and continents, Environ. Res. Lett., 5, 034007, https://doi.org/10.1088/1748-9326/5/3/034007, 2010.

Yli-Juuti, T., Mielonen, T., Heikkinen, L., Arola, A., Ehn, M., Isokääntä, S., Keskinen, H.-M., Kulmala, M., Laakso, A., Lipponen, A., Luoma, K., Mikkonen, S., Nieminen, T., Paasonen, P., Petäjä, T., Romakkaniemi, S., Tonttila, J., Kokkola, H., and Virtanen, A.: Significance of the organic aerosol driven climate feedback in the boreal area, Nat. Commun., 12, 5637, https://doi.org/10.1038/s41467-021-25850-7, 2021.

Zhang, C., Hai, S., Gao, Y., Wang, Y., Zhang, S., Sheng, L., Zhao, B., Wang, S., Jiang, J., Huang, X., Shen, X., Sun, J., Lupascu, A., Shrivastava, M., Fast, J. D., Cheng, W., Guo, X., Chu, M., Ma, N., Hong, J., Wang, Q., Yao, X., and Gao, H.: Substantially positive contributions of new particle formation to cloud condensation nuclei under low supersaturation in China based on numerical model improvements, Atmos. Chem. Phys., 23, 10713–10730, https://doi.org/10.5194/acp-23-10713-2023, 2023.

Zheng, G., Wang, Y., Wood, R., Jensen, M. P., Kuang, C., McCoy, I. L., Matthews, A., Mei, F., Tomlinson, J. M., Shilling, J. E., Zawadowicz, M. A., Crosbie, E., Moore, R., Ziemba, L., Andreae, M. O., and Wang, J.: New particle formation in the remote marine boundary layer, Nat. Commun., 12, 527, https://doi.org/10.1038/s41467-020-20773-1, 2021.